IEEE Access
Multidisciplinary | Rapid Review | Open Access Journal

Robotic Assistance for Physical Human-Robot Interaction Using a Fuzzy RBF Hand Impedance Compensator and a Neural Network Based Human Motion Intention Estimator

SHIH-HSUAN CHIEN [1], JYUN-HSIANG WANG [1], AND MING-YANG CHENG [1], MEMBER, IEEE

[1]Department of Electrical Engineering, National Cheng Kung University, Tainan, Taiwan

Corresponding author: Ming-Yang Cheng (e-mail: mycheng@mail.ncku.edu.tw).

This work was supported in part by the Industrial Technology Research Institute and the Ministry of Science and Technology, Taiwan, under Grant No. MOST 105-2221-E-006-105-MY3.

ABSTRACT This paper proposes a robotic assistance control scheme for intuitive teaching tasks by integrating the motion intention of human and real-time hand impedance compensation based upon a fuzzy RBF (Radial Basis Function) compensator. The motion intention of a human is estimated using a feedforward neural network. The parameters of the proposed fuzzy RBF hand impedance compensator are adjusted by considering hand impedance and robot dynamics. Three robotic assistance control schemes are compared: 1) robot without an impedance compensator; 2) robot with a constant-parameter impedance compensator; 3) robot with a fuzzy RBF hand impedance compensator. Several experiments have been conducted to verify the effectiveness of the proposed approach by comparing the contour error, exerted force and task time spent on teaching tasks. Experimental results indicate that the proposed fuzzy RBF hand impedance compensator has the best assistance results among the tested robotic assistance control schemes.

INDEX TERMS robot manipulator, impedance compensator, physical human-robot interaction

I. INTRODUCTION

Physical human-robot interaction is a crucial issue in human-robot collaboration that is becoming more and more popular across many applications. In particular, application scenarios such as rehabilitation [1] or intuitive teach pendants [2],[3] require the collaborative work of humans and robots. During these tasks, human operators need to interact with the robot for a long period of time. Impedance control [4]-[6] or admittance control [7]-[9] is usually implemented to ensure compliant motion of the robot. Some tasks such as manual welding [10] or laparoscopic training [11] require the robot to perform with precision and minimize energy consumption of the operator. Therefore, variable admittance [12],[13] or assistive schemes [14]-[18] are applied to assist the human. To emulate the human decision-making process during teach tasks, fuzzy logic related methods are commonly used when tuning variable admittance parameters or compensator gains [19]-[22].

Estimation of human motion intention is also a crucial topic for improving human-robot collaboration. Understanding such motion intention can facilitate tasks being carried out more smoothly. In [23], by estimating indirect intention, a force guidance method is suggested to enable a robot to both follow and guide a human. In [25], a smooth Kalman filter is used to estimate human hand movements for an impedance compensator. In [26], the motion intention of a human as represented by the change of the interaction force is estimated by the change of control effort. Neural networks (NNs) is also a popular estimation method that has excellent approximation ability [27]. In [24], a neural network-based method uses an RBF to estimate the motion intention and define it as the desired trajectory for an adaptive admittance controller. In particular, the weights of NNs are adjusted online so that even when human motion intention changes, the estimation accuracy is still guaranteed.

Knowing the motion intention of a particular human can facilitate the design of assistive schemes. The design of these assistive schemes also requires the measurement of human hand impedance. This is due to each person having different dynamic characteristics which should be taken into consideration. Electromyography (EMG) signals can be used for measuring human hand impedance [28],[29]. In [28], the human tutor's stiffness is estimated based on limb surface EMG signals; Gaussian mixture regression (GMR) is then utilized to generate the expected impedance variables. In [29], a variable admittance scheme/compensator is implemented to

enhance control performance. However, the acquisition of EMG signals requires the use of additional sensors and equipment. In contrast, some methods focus on the measurement of human hand impedance by introducing position disturbance [30] or force disturbance [31],[32] during the interaction between human operators and robots. In [31], the end-point impedance is measured across dominant and non-dominant hands by the force disturbance method and a directional damping scheme is developed for robotic assistance. In [32], the issue of measurement of hand impedance of professional and novice welders during manual welding is investigated. There are also studies that do not take external disturbance into consideration. In [33], a variable impedance controller is proposed to render the collaborative robot stable while performing a calligraphy task. In [17], a dropping mass device is used to estimate the hand impedance, for which a novel algorithm using frequency analysis and a force sensor is proposed.

Most of the existing literatures on impedance compensators have discussed issues accompanying the estimation of human hand impedance offline or involving the use of other equipment. However, during teaching tasks, the values of human hand impedance parameters might not remain unchanged. For example, a human operator would need to enhance arm stiffness as it is required in order to precisely move along a specific trajectory. Therefore, an impedance compensator that is able to adapt to these changes would be desirable.

In this paper, a fuzzy RBF hand impedance compensator that uses a force sensor mounted on the robot's end-effector is proposed. The proposed approach exploits fuzzy logic to emulate the human decision-making process during teaching tasks and integrates the radial basis function neural networks (RBFNN) and the fuzzy c-means algorithm for calculation. The use of fuzzy c-means allows the network to provide a more accurate representation of real-life situations, where an input can have finite non-zero membership of two or more classes. One of the aims of this paper is to reduce the force exerted by humans during teaching tasks by a compensation force in the intended direction of movement. In particular, the motion intention of a human is estimated by a feedforward neural network, while hand impedance is estimated by using a fuzzy RBF approach so as to obtain optimal compensator parameters for different hand impedances.

We highlight the contributions of this paper as follows: the estimation results of hand impedance and motion intention are integrated to produce a compensation force. The proposed approach aims at dealing with the drawback of the conventional approach of being unable to adapt to different hand impedance situations online. Bode plot analysis is exploited to facilitate the design of parameter values for the proposed fuzzy RBF hand impedance compensator. Two experiments are carried out to assess the performance of the proposed approach. A 6-DOF industrial robot is used as the experimental platform. The first experiment is to train the connection weights of the neural network-based human intention estimator. The second experiment is to find the optimum parameter values under three different hand impedance conditions. Experimental results show that the proposed fuzzy RBF hand impedance compensator has the best performance in reduction of exerted force and task time among the control schemes tested in the experiment.

The remainder of this paper is organized as follows. Section II briefly reviews conventional hand impedance measurement methods and lays out the problem discussed in this paper. The proposed fuzzy RBF hand impedance compensator and the neural network based motion intention estimator is introduced in Section III. Experimental results are shown in Section IV. Conclusions are given in Section V.

II. PROBLEM DESCRIPTION

A. OFFLINE HAND IMPEDANCE MEASUREMENTS

The force disturbance based approach for hand impedance measurement has received much attention recently [31]. Hand impedance is measured while the subjects are carrying out a teaching task. Force disturbance is exerted for a short period of time. Deviations in position, velocity and acceleration during this short period of time are considered to be a result of force disturbances. The relationship between deviation and force disturbance can be modeled as a mass-spring-damper system. Least-squares methods can then be applied to calculate the human mass M_H, spring constant K_H and damping coefficient D_H, as described in (1) and (2).

$$f_e = M_H \ddot{x}_e + D_H \dot{x}_e + K_H x_e \tag{1}$$

$$\begin{aligned} f_e(t) &= -(F_{ext}(t) - F_{ext}(t_d)),\ t_d < t \le t_w \\ x_e(t) &= x(t) - x(t_d),\ t_d < t \le t_w \end{aligned} \tag{2}$$

where f_e is the force disturbance, while t_d and t_w represent the starting and ending time of the disturbance, respectively; x_e, $\dot{x}_e$, $\ddot{x}_e$ represent position deviation, velocity deviation and acceleration deviation, respectively.

B. PROBLEMS TO BE SOLVED

The obtained hand impedance information can be used as the basis for designing impedance compensators. However, the design of optimal compensator parameters would be a difficult task, since each user would need to undergo offline experiments before executing a teaching task. Furthermore, the parameter values of hand impedances of a user might change during teaching tasks due to different precision requirements. Compensator parameters with constant values would not be sufficient. Therefore, online hand impedance estimation can facilitate the compensator design.

III. FUZZY RBF HAND IMPEDANCE COMPENSATOR

Fig. 1 shows the block diagram of the proposed fuzzy RBF hand impedance compensator. The actual velocity and position of the robot are represented by V and x, respectively. In ideal cases, the input to the impedance control scheme is the human force measured by a force sensor. However, the measurement results of a force sensor may not faithfully represent the human's motion intention due to hand tremor

This article has been accepted for publication in a future issue of this journal, but has not been fully edited. Content may change prior to final publication. Citation information: DOI 10.1109/ACCESS.2021.3111875, IEEE Access

or force feedback between the hand and the force sensor. The original human motion may then be affected by the human hand impedance. In order to cope with this difficulty, a fuzzy RBF impedance compensator based on real-time human hand impedance and human intention estimation is proposed in this paper to improve the accuracy of the control loop and minimize the force spent. As indicated in Fig. 1, in the proposed approach, the inputs to the admittance control scheme consist of human force measured by the force sensor and compensation force provided by the impedance compensator. The output of the admittance control scheme is used as the desired velocity command V_d to the robot. Details of the proposed fuzzy RBF hand impedance compensator are elaborated upon in the following:

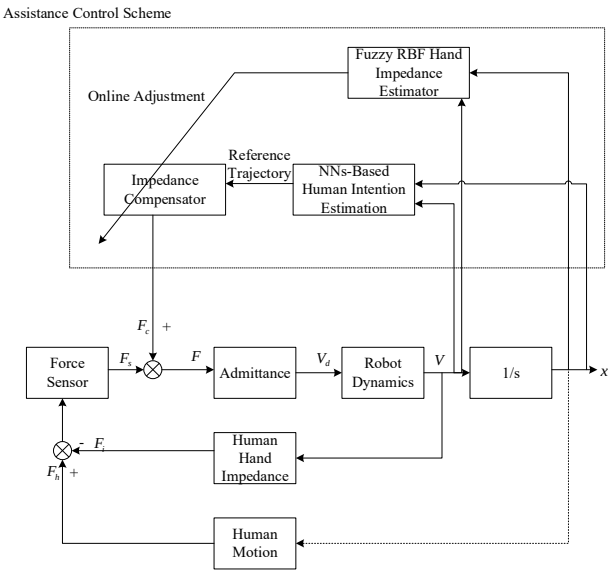

FIGURE 1. Block diagram of the proposed fuzzy RBF hand impedance compensation scheme.

A. Admittance Control

In general, the goal of an admittance control scheme for an end-effector is to control its motion so that the dynamics of the end-effector can be described as a mass-damper system with *m, c* representing the virtual mass and damping coefficients, respectively. In particular, the dynamic model of the mass-damper system can be described by (3):

$$m\ddot{x} + c\dot{x} = F_s \tag{3}$$

where $\dot{x}$ and $\ddot{x}$ represent the velocity and acceleration in the operational space, respectively; F_s is the external force measured by the force sensor. The desired velocity $V_d = \dot{x}_d$ can be approximated using a discrete time equation described by (4), where T_s denotes the sampling time.

$$V_d(k) = \frac{F_s(k) - c\dot{x}_d(k-1)}{m} T_s + \dot{x}_d(k-1) \tag{4}$$

B. Fuzzy RBF HAND IMPEDANCE ESTIMATOR

Fig. 2 shows the schematic diagram of the human hand impedance model that is described as a mass-damper-spring system, where M_H, D_H and K_H are the mass, damping and stiffness coefficients of the human hand, respectively. In particular, the relationship between the external force and the position of the human hand in the operational space can be described by (5):

$$F_i = M_H\ddot{x} + D_H\dot{x} + K_H x \tag{5}$$

where $\ddot{x}, \dot{x}, x$ represent the acceleration, velocity and position of the human hand, which are equivalent to the acceleration, velocity and position of the robot's end-effector during teaching tasks. Due to the fact that damper and spring parameters usually dominate the hand impedance model, the hand mass is not estimated online.

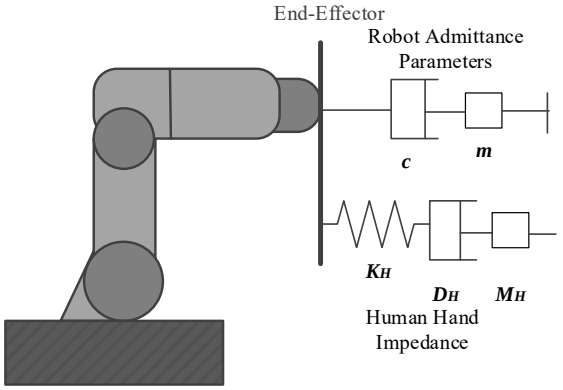

FIGURE 2. Schematic diagram of the human hand impedance model

According to Hooke's law, the stiffness coefficient can be estimated from the ratio of force variation to position variation. The damping coefficient can be estimated from the ratio of force variation to velocity variation. In addition, the variations in force, velocity and position of the human hand are calculated using (6)~(8)

$$\Delta F(t) = F_s(t) - F_s(t - T_s) \tag{6}$$

$$\Delta\dot{x}(t) = \dot{x}(t) - \dot{x}(t - T_s) \tag{7}$$

$$\Delta x(t) = x(t) - x(t - T_s) \tag{8}$$

where ΔF, $\Delta\dot{x}$ and Δx represent the force variation, velocity variation and position variation, respectively.

Therefore, the first input of the fuzzy RBF loop—stiffness coefficient—is the ratio of force variation to position variation; the second input—the damping coefficient—is the ratio of force variation to velocity variation. In this paper, the damping and stiffness coefficients are obtained from the offline hand impedance measurement. With these measurements and using (6)~(8), one can obtain three data sets of variations in force, velocity and position of the human hand. In order to estimate the stiffness coefficient and the damping coefficient, the ratio of force variation to position variation and the ratio of force variation to velocity variation at each sampling time are calculated using the three obtained data sets. Theoretically, we can directly calculate the stiffness and damping coefficients online by using (6)~(8). However, in practice, the data obtained online would be severely influenced by measurement noise; as such, accurate results would be difficult to obtain. This paper employs fuzzy

RBF methods to deal with this problem. By using fuzzy c-means [34], the calculated ratios of force variation to position variation and force variation to velocity variation at each sampling time are divided into three clusters—high hand impedance, medium hand impedance and low hand impedance.

As defined by (9), c_{11}, c_{21}, c_{31} are the three centers of high, medium and low hand stiffness, while c_{12}, c_{22}, c_{32} are the three centers of high, medium and low hand damping.

$$\begin{cases} c_{11} = [\dfrac{\Delta F}{\Delta x}]_{high},\ c_{12} = [\dfrac{\Delta F}{\Delta \dot{x}}]_{high} \\ c_{21} = [\dfrac{\Delta F}{\Delta x}]_{medium},\ c_{22} = [\dfrac{\Delta F}{\Delta \dot{x}}]_{medium} \\ c_{31} = [\dfrac{\Delta F}{\Delta x}]_{low},\ c_{32} = [\dfrac{\Delta F}{\Delta \dot{x}}]_{low} \end{cases} \tag{9}$$

The membership function $u_k^{(j)}$ of the jth input (i.e. stiffness coefficient and damping coefficient) is then acquired first by calculating the distance of the input to the three centers using (10).

$$u_k^{(j)} = \frac{h_k^{(j)}}{\sum_{i=1}^{3} h_i^{(j)}},\ 1 \le k \le 3 \tag{10}$$

where $h_k^{(j)} = (\dfrac{1}{d_{kj}})^{(2/n-1)}$

where d_{kj} is the distance between the j^{th} input and the k^{th} center, n is the fuzzifier and the number of hidden nodes is 3. Then the output of the fuzzy RBF $y_i^{(j)}$ for each j^{th} input is calculated using (11).

$$y_i^{(j)} = \sum_{k=1}^{3} W_{ik}^{(j)} u_k^{(j)},\ 1 \le i \le 3 \tag{11}$$

where $W_{ik}^{(j)}$ is the weight between two neurons for each jth input. Note that the weight is randomly set in the range of 0-0.5 initially and it is adjusted online by the cost function E and the learning rate η. In particular, the adjustment $\Delta W_{ik}^{(j)}$ to the weight $W_{ik}^{(j)}$ is described by (12):

$$\Delta W_{ik}^{(j)} = \frac{\eta}{\sum_{i=1}^{3} h_i^{(j)}} \cdot E \cdot h_k^{(j)} \tag{12}$$

Since the objective of the impedance compensator is to control the end-effector of the robot to move toward the intended position of the user and minimize the force spent, the cost function is thus set as follows:

$$E = \frac{1}{2}(\mu_{\max})^2 \tag{13}$$

$$\mu_{\max} = \frac{(F - F_{\max})^{(-2/n-1)}}{(F - F_{\max})^{(-2/n-1)} + (F - F_{\text{medium}})^{(-2/n-1)} + (F - F_{\min})^{(-2/n-1)}} \tag{14}$$

where $\mu_{\max}$ is the membership function of the maximum force, while $F_{\max}$, F_{medium}, and $F_{\min}$ are the maximum, medium and minimum force during the task, respectively, which can be set by the designer.

After acquiring the output $y_i^{(j)}$ for each input, the center of area method described by (15) is used for defuzzification:

$$[K_H \ D_H]^{(j)} = \frac{1}{\sum_{i=1}^{3} y_i^{(j)}} \left[\sum_{i=1}^{3} y_i^{(j)} \cdot c_{i1} \quad \sum_{i=1}^{3} y_i^{(j)} \cdot c_{i2} \right] \tag{15}$$

where c_{i1} are the three centers of high, medium and low hand stiffness, and c_{i2} are the three centers of high, medium and low hand damping, as described by (9). In this paper, the hand impedance (i.e. K_H and D_H) for each j^{th} input is estimated online using (15).

C. IMPEDANCE COMPENSATOR DESIGN

The values of compensator parameters are adjusted based on human hand impedance during the teaching task. It is assumed that the admittance control scheme adopted in this paper can be described as a linear mass-damper system. The human hand impedance model, and the impedance compensator in Fig. 1 are also set as linear mass-spring systems, described by (16), (17) and (18), respectively [17]:

$$\frac{V_d(s)}{F(s)} = \frac{1}{ms + c} \tag{16}$$

$$\frac{F_i(s)}{V(s)} = \frac{M_H s^2 + D_H s + K_H}{s} \tag{17}$$

$$\frac{F_c(s)}{V(s)} = \frac{M_c s^2 + D_c s + K_c}{s} \tag{18}$$

where M_c, D_c and K_c are the mass, damping and stiffness coefficients of the impedance compensator, respectively.
In addition, the robot controller is assumed to be ideal. Therefore, the transfer function for the robot dynamics in Fig. 1 is set to be 1. The transfer functions for the robotic system without and with the impedance compensator can be described by (19) and (20), respectively [17].

$$G_c = \frac{X(s)}{F_h(s)} = \frac{1}{(m + M_H)s^2 + (c + D_H)s + K_H} \tag{19}$$

$$G_o = \frac{X(s)}{F_h(s)} = \frac{1}{(m + M_H - M_c)s^2 + (c + D_H - D_c)s + (K_H - K_c)} \tag{20}$$

In this paper, the parameter values for high, medium and low hand impedance are chosen such that the resulting Bode plots have large magnitude and small phase lag.

D. ESTIMATION OF MOTION INTENTION OF A HUMAN

This article has been accepted for publication in a future issue of this journal, but has not been fully edited. Content may change prior to final publication. Citation information: DOI 10.1109/ACCESS.2021.3111875, IEEE Access

This paper proposes a neural network (NN) based human motion intention estimator to predict the trajectory of hand movement with the aim of facilitating the design of a hand impedance compensator. The estimated hand trajectory is used as a reference for the hand impedance compensator so that the end-effector can move along the intended trajectory.

The motion intention x_{Hd} described by (21) is mainly influenced by human force F, actual velocity $\dot{x}$ and position x [24].

$$x_{Hd} = G(F, x, \dot{x}) \tag{21}$$

In this paper, a feedforward neural network with one hidden layer is used for estimating human motion intention. As described by (22), (23) and (24), L_1 is the input layer; L_2 is the hidden layer; L_3 is the output layer; w_2 and w_3 are the connection weights between the layers; B_2 and B_3 are the biases; and $F(\bullet)$ is the sigmoid activation function.

$$L_1 = [F \quad x \quad \dot{x}] \tag{22}$$

$$L_2 = F(L_1 \times w_2 + B_2) \tag{23}$$

$$L_3 = L_2 \times w_3 + B_3 \tag{24}$$

In this paper, backpropagation is employed in training the feedforward neural network and the cost function used in the neural network training is described by (25):

$$E = 0.5 \times \sum (L_3 - x_{Hd})^2 \tag{25}$$

E. STEPS FOR FUZZY RBF HAND IMPEDANCE COMPENSATOR

The schematic diagram of the proposed fuzzy RBF hand impedance compensator is illustrated in Fig.3. The following details the steps for implementing the proposed fuzzy RBF hand impedance compensator.

Step 1: The user executes the teaching task by dragging the robot's end-effector.

Step 2: Admittance control is applied to set the robot in a compliant motion mode.

Step 3: Human intention and hand impedance are estimated by a feedforward neural network and a fuzzy RBF, respectively.

Step 4: Reference trajectories obtained from the human intention estimator and the proposed fuzzy RBF hand impedance compensator are used to calculate the assistive compensation force.

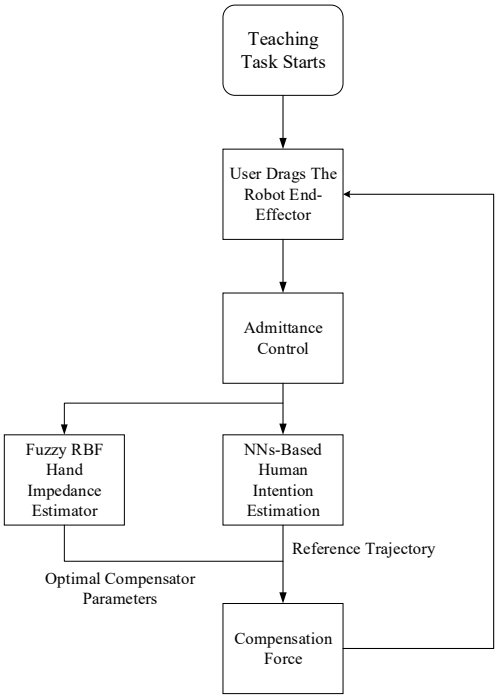

FIGURE 3. The schematic diagram of the proposed fuzzy RBF hand impedance compensator used in the teaching task

IV. EXPERIMENTAL RESULTS

The fuzzy RBF hand impedance compensator designed in this paper is implemented in an intuitive teaching task of a 6-DOF industrial robot manipulator manufactured by ITRI, as shown in Fig. 4. A 6-axis force/torque sensor is mounted on the end-effector of the manipulator to measure the contact force between the human operator and the end-effector, while the angle of each joint is indirectly measured using a built-in encoder of the servomotor and the gear ratio between the servomotor and the harmonic drive. During the experiments, human operators are asked to hold the end-effector of the robot and move along different desired trajectories as shown in Fig. 5.

Three different experiments—NN-based motion intention estimation, off-line hand impedance measurements, and fuzzy RBF hand impedance compensator in teaching tasks—are conducted. The robot with the proposed fuzzy RBF hand impedance compensator is compared to the one with a constant impedance compensator and the one without any impedance compensator.

This article has been accepted for publication in a future issue of this journal, but has not been fully edited. Content may change prior to final publication. Citation information: DOI 10.1109/ACCESS.2021.3111875, IEEE Access

FIGURE 4. 6-DOF industrial robot manipulator manufactured by ITRI

FIGURE 5. A human operator holds the end-effector and moves along a desired trajectory

A. NN-based motion intention estimation

The trajectories used for training and testing are each recorded under an admittance controlled intuitive teaching task. MATLAB is then used to train the weights and biases of the feedforward neural network. Next, the NN-based motion intention estimator is tested to validate its feasibility. An oval trajectory is used as the training data and the training results are shown in Fig. 8 and Fig. 9. The testing data is a rectangular trajectory, for which Fig. 7 and Fig. 8 show the desired and actual estimated trajectory of the testing data on the x-axis and y-axis, respectively. Experimental results indicate that the NN-based motion intention estimator exhibits satisfactory results and therefore can be implemented on the proposed fuzzy RBF hand impedance compensator.

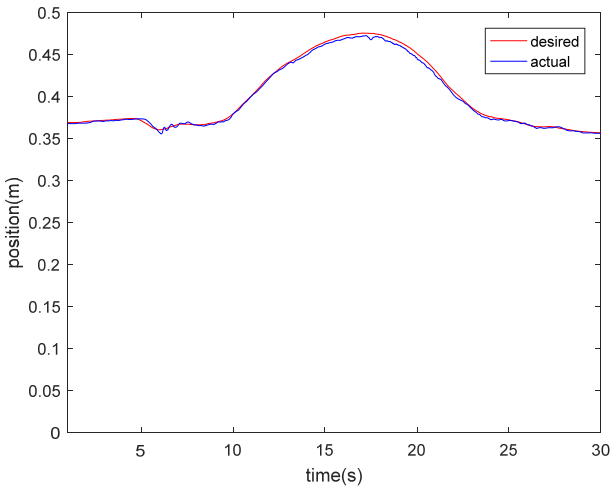

FIGURE 6. Desired and actual estimated trajectory of the training data on the X-axis

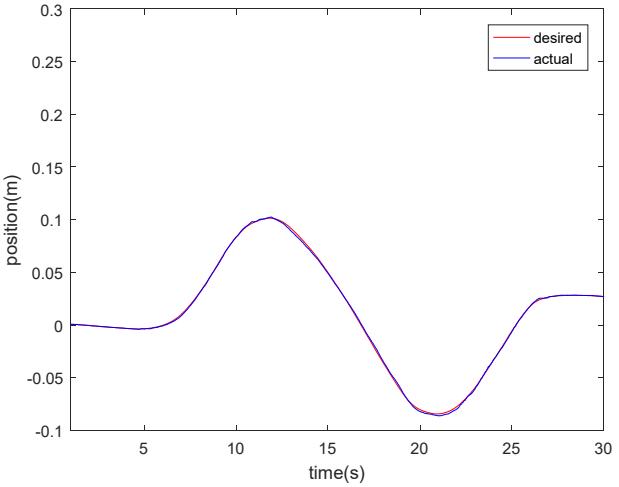

FIGURE 7. Desired and actual estimated trajectory of the training data on the Y-axis

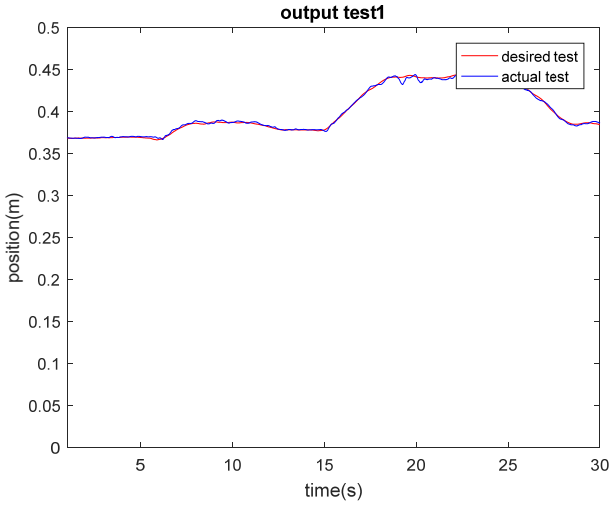

FIGURE 8. Desired and actual estimated trajectory of the testing data on the X-axis

This article has been accepted for publication in a future issue of this journal, but has not been fully edited. Content may change prior to final publication. Citation information: DOI 10.1109/ACCESS.2021.3111875, IEEE Access

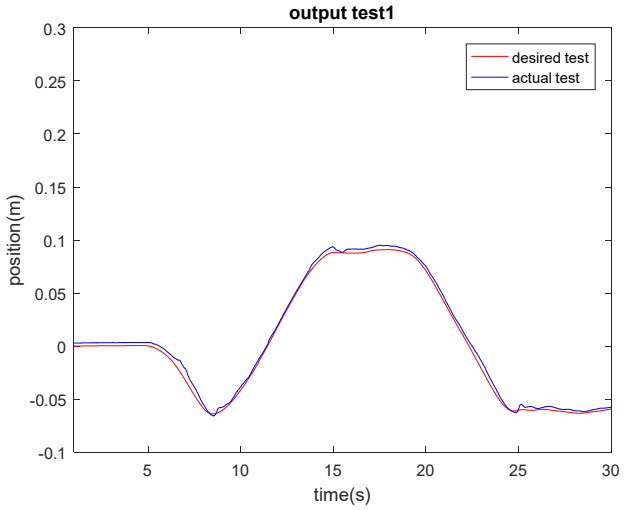

FIGURE 9. Desired and actual estimated trajectory of the testing data on the Y-axis

B. Off-line hand impedance measurements

Seven male and two female participants aged 20-25 each conducted the hand impedance experiment five times. While dragging the end-effector of the robot to move along a circle trajectory, a force disturbance that lasts for 500 ms is applied in the 7-8 second region on the X-axis and 12-13 second region on the Y-axis, as shown in Fig. 10. Four sets of data are used in the least-squares method to estimate the human hand impedance. The other set of data is used as the validation data to compare with the re-estimated force by the hand impedance results, as shown in Fig. 11 and Fig. 12. The results of the hand impedance estimation are categorized into high, medium and low groups, as shown in Table I.

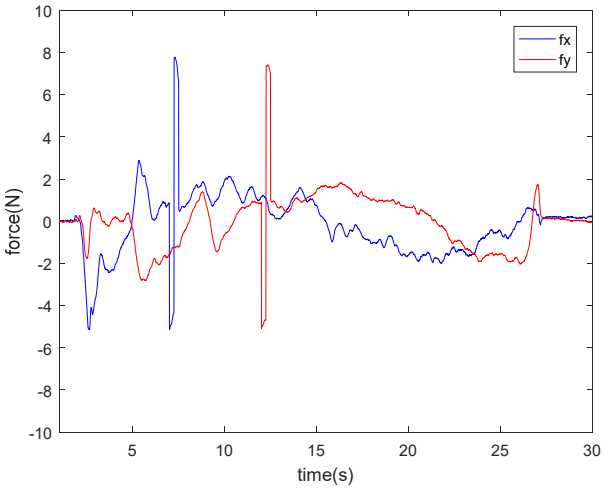

FIGURE 10. Force data during the experiment

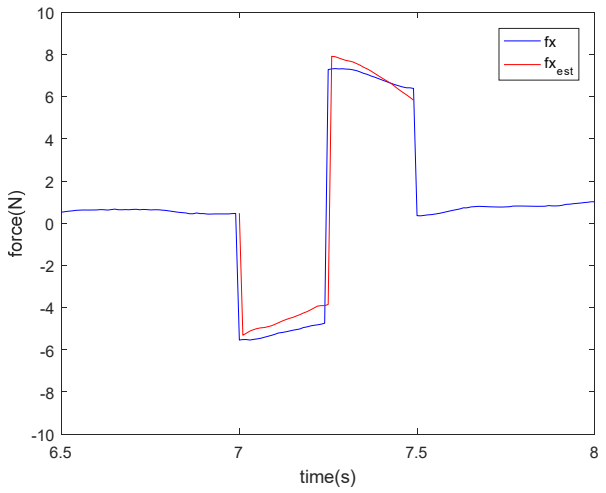

FIGURE 11. Comparison of re-estimation results and actual force on the X-axis

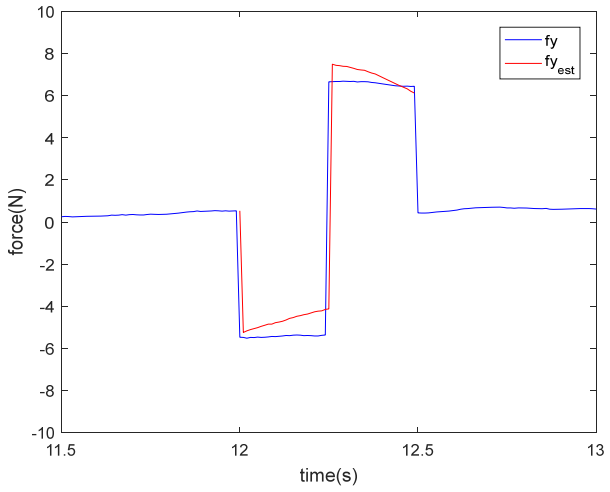

FIGURE 12. Comparison of re-estimation results and actual force on the Y-axis

TABLE I. AVERAGES OF ESTIMATED HAND IMPEDANCE OF THREE GROUPS

Group	Damping (Ns/m)	Stiffness (N/m)
	X-axis	
Low	15	5
Medium	28	33
High	40	60
	Y-axis	
Low	18	10
Medium	28	28
High	40	45

C. Fuzzy RBF HAND IMPEDANCE COMPENSATOR

The transfer function for the robotic system with the impedance compensator is exploited to determine the parameter values. In particular, the Bode plots of well-designed parameters for high, medium and low impedance groups and the ones with constant parameters/without compensators are compared. The group of parameters that

This article has been accepted for publication in a future issue of this journal, but has not been fully edited. Content may change prior to final publication. Citation information: DOI 10.1109/ACCESS.2021.3111875, IEEE Access

yield the largest magnitude and smallest phase lag in the Bode plot are selected as the well-designed hand impedance parameter values for the impedance compensator. As an example, Fig. 13 shows the comparison of the three kinds of compensators under the condition of low damping and medium stiffness.

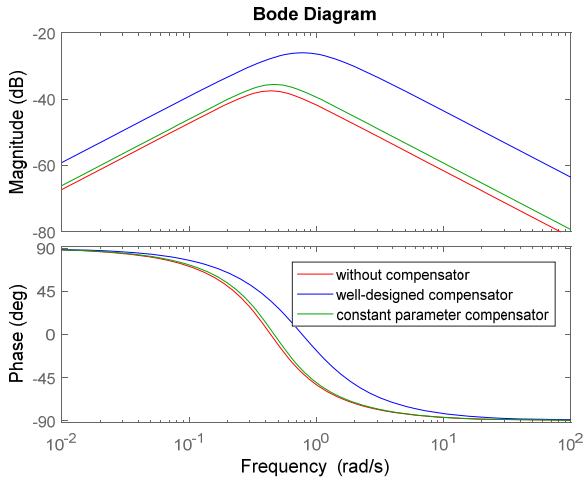

FIGURE 13. Bode plots for three cases of hand impedance compensators

In Fig. 13, the red line represents the robotic system without a hand impedance compensator, the blue line represents the robotic system with well-designed hand impedance compensator parameters, and the green line represents the robotic system with constant hand impedance compensator parameters. Clearly, the blue line has the largest magnitude and smallest phase lag, indicating that the well-designed hand impedance compensator parameters yield the best performance among the three tested cases. The well-designed hand impedance parameter values for each group are shown in Table II.

TABLE II. COMPENSATOR PARAMETERS THAT YIELD THE BEST PERFORMANCE

Hand Impedance	Values of Compensator Parameters	
High	D_c=40	K_c=4
Medium	D_c=60	K_c=14
Low	D_c=70	K_c=50

The three groups of damping and stiffness coefficients for the Fuzzy RBF hand impedance estimator are obtained from the offline hand impedance measurements, as shown in Table I. The maximum force, medium force and minimum force essential in (14) are set as shown in Table III. Next, the hand impedance estimated by the fuzzy RBF estimator is compared with that obtained using an offline method to ensure the estimation results are in the same hand impedance group, as shown in Table IV and Table V. Clearly, the fuzzy RBF hand impedance compensator provides correct hand impedance estimation results that fall within the same group as those obtained using an offline method.

TABLE III. MAXIMUM, MEDIUM AND MINIMUM FORCE

Criteria	Force(N)
$F_{\min}$	1
F_{medium}	2
$F_{\max}$	4

TABLE IV. ESTIMATION OF DAMPING PARAMETER

Offline Estimation	Fuzzy RBF Estimation	Same Group?
Low (5-20)	16.9	y
Medium (21-35)	28.39	y
High (35-40)	38.06	y

TABLE V. ESTIMATION OF STIFFNESS PARAMETER

Offline Estimation	Fuzzy RBF Estimation	Same Group?
Low (1-10)	7.76	y
Medium (10-55)	11.5	y
High (55-100)	56.1	y

Eight subjects in the age range of 20-25 conducted a circle drawing task under three different cases—without an impedance compensator, with a constant parameter impedance compensator, and with a fuzzy RBF hand impedance compensator. Fig. 14 shows the results of the circle-drawing task for three different cases. In particular, the red solid line represents the case with a fuzzy RBF hand impedance compensator; the blue solid line represents the case with a constant parameter impedance compensator; the green solid line represents the case without an impedance compensator; and the dashed line represents the reference circle trajectory. Table VI shows a comparison of the circle-drawing task with and without the impedance compensator. Clearly, the impedance compensator improves circle-drawing accuracy.

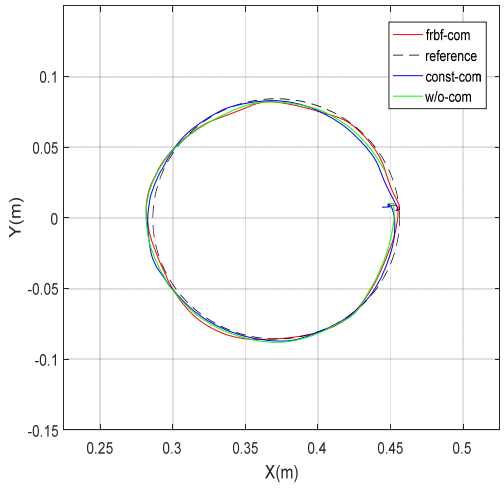

FIGURE 14. Circle-drawing results

This article has been accepted for publication in a future issue of this journal, but has not been fully edited. Content may change prior to final publication. Citation information: DOI 10.1109/ACCESS.2021.3111875, IEEE Access

TABLE VI. CONTOUR ERROR COMPARISONS OF CIRCLE-DRAWING

Data	RMS of contour Error (m)
Without Compensator	0.0030
With Compensator	0.0027

The mean force and task time for different cases are also compared. To obtain meaningful data, only the results that have a circle-drawing error of smaller than 0.05m are used for comparison. Table VII shows comparisons of three different cases, while Table VIII shows the percentage of reduction in exerted force and task time for the cases of constant parameters and the fuzzy RBF hand impedance compensator. Fig. 15 shows the exerted force for different cases. In particular, the blue line represents the case with a fuzzy RBF hand impedance compensator; the red line represents the case with a constant parameter impedance compensator; the black line represents the case without an impedance compensator.

TABLE VII. COMPARISONS OF DIFFERENT METHODS

Data	X-axis Mean Force (N)	Y-axis Mean Force (N)	Task Time (s)
Without Compensator	1.62	1.34	28.09
Constant Parameter Compensator	1.49	1.21	26.58
Fuzzy RBF Compensator	1.27	1.01	24.59

TABLE VIII. COMPARISONS OF REDUCTION IN EXERTED FORCE AND TASK TIME

Compensator	X-axis Exerted Force Reduction	Y-axis Exerted Force Reduction	Task Time Reduction
Constant	7.97%	10.67%	5.37%
FRBF	16.7%	15%	13.53%

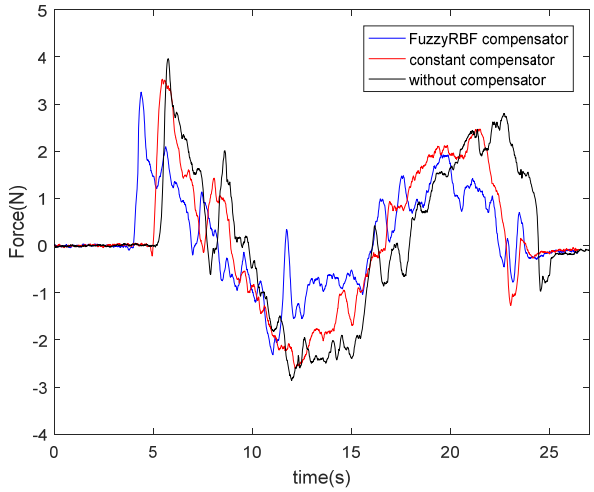

FIGURE 15. Recorded force in teaching tasks for three methods

According to the results shown in Table VI, Table VII and Fig. 15, clearly the one with a fuzzy RBF hand impedance compensator demonstrates the best performance in force reduction and time spent on teaching tasks. On both the X-axis and Y-axis, it saves at least 15% of the exerted force and the task time reduction is more than 10%. Therefore, we can conclude that the proposed fuzzy RBF hand impedance compensator has the best assistive results among the three tested methods.

V. CONCLUSION

In this paper, a fuzzy RBF hand impedance compensator is proposed to assist human users when conducting intuitive teaching tasks. Due to the fact that different positions in the teaching trajectory require different velocity and force, human users have to adjust their hand impedance during tasks. Therefore, it would be vital to change the impedance compensator parameters in real time. Also, it is essential to integrate the motion intention of the user in the design of the compensator so that the compensation force is in the intended direction of the user. To this end, this paper proposes a fuzzy RBF approach to estimate hand impedance and the estimation accuracy is verified by offline measurements. The proposed assistive scheme reduces the effects of hand tremor and improves the performance of admittance control. By combining an NN-based motion intention estimator with the fuzzy RBF hand impedance compensator, accuracy of teaching tasks can be further improved. In particular, the proposed approach can estimate human hand impedance in real time and reduce the force spent by the user through compensation in the intended direction. It performs better than the commonly used constant impedance compensator.

ACKNOWLEDGMENT

The authors would like to thank the Industrial Technology Research Institute and the Ministry of Science and Technology, Taiwan, for support of this research under Grant No. MOST 105-2221-E-006-105-MY3.

REFERENCES

[1] G. Sebastian, Z. Li, V. Crocher, D. Kremers, Y. Tan, and D. Oetomo, "Interaction Force Estimation Using Extended State Observers: An Application to Impedance-Based Assistive and Rehabilitation Robotics," *IEEE Robot. Automat. Letters,* vol. 4, no. 2, pp. 1156-1161, 2019.

[2] P. D. Labrecque, T. Laliberte, S. Foucault, M. E. Abdallah, and C. Gosselin, "uMan: A Low-Impedance Manipulator for Human–Robot Cooperation Based on Underactuated Redundancy," *IEEE/ASME Trans. Mechatronics,* vol. 22, no. 3, pp. 1401-1411, 2017.

[3] F. Ficuciello, L. Villani, and B. Siciliano, "Variable Impedance Control of Redundant Manipulators for Intuitive Human–Robot Physical Interaction," *IEEE Trans. Robot.,* vol. 31, no. 4, pp. 850-863, 2015.

[4] N. Hogan, "Impedance Control: An Approach to Manipulation: Part I: Theory," *J. Dyn. Syst., Meas., Control, vol. 107, no.1, pp. 1-24, 1985.*

[5] H. Cao, X. Chen, Y. He and X. Zhao, "Dynamic Adaptive Hybrid Impedance Control for Dynamic Contact Force Tracking in Uncertain Environments," *IEEE Access*, vol. 7, pp. 83162-83174, 2019.

[6] S. -H. Chien, J. -H. Wang and M.-Y. Cheng, "Performance comparisons of different observer-based force-sensorless approaches for impedance control of collaborative robot manipulators," in *Proc. 3rd IEEE Int. Conf. Industrial Cyber Physical Systems (ICPS)*, Tampere, Finland, 2020, pp. 326-331.

[7] Z. Li, B. Huang, Z. Ye, M. Deng, and C. Yang, "Physical Human–Robot Interaction of a Robotic Exoskeleton By Admittance Control," *IEEE Trans. Ind. Electron.*, vol. 65, no. 12, pp. 9614-9624, 2018.

[8] J. Bae, K. Kim, J. Huh and D. Hong, "Variable Admittance Control With Virtual Stiffness Guidance for Human–Robot Collaboration," *IEEE Access*, vol. 8, pp. 117335-117346, 2020.

[9] C. -Y. Liou, J. -H. Wang, S. -H. Chien, M. -Y. Cheng and C. -Y. Tai, "Compliance Control and External Force Estimation of 6-DOF Industrial Robots," in *Proc. Int. Automatic Control Conf. (CACS)*, Hsinchu, Taiwan, 2020, pp. 1-5.

[10] M. S. Erden and A. Billard, "Hand impedance measurements during interactive manual welding with a robot," *IEEE Trans. Robot.*, vol. 31, no. 1, pp. 168-179, Feb. 2015.

[11] H. Tugal, B. Gautier, M. Kircicek and M. S. Erden, "Hand-Impedance Measurement During Laparoscopic Training Coupled with Robotic Manipulators," in *Proc. IEEE/RSJ Int. Conf. Intell. Robots Syst.*, Madrid, 2018, pp. 4404-4410.

[12] F. Dimeas and N. Aspragathos, "Fuzzy learning variable admittance control for human-robot cooperation," in *Proc. IEEE/RSJ Int. Conf. Intell. Robots Syst.*, pp. 4770–4775, 2014.

[13] F. Dimeas and N. Aspragathos, "Reinforcement learning of variable admittance control for human-robot co-manipulation,"in *Proc. IEEE/RSJ Int. Conf. Intell. Robots Syst.*, 2015, pp. 1011–1016.

[14] C.-J. Chen, M.-Y. Cheng, and K.-H. Su, "Observer-based impedance control and passive velocity control of power assisting devices for exercise and rehabilitation," in *Proc. 39th Annual Conf. IEEE Ind. Electron. Society*, pp. 6502-6507, 2013.

[15] H. Modares, I. Ranatunga, F. L. Lewis, and D. O. Popa, "Optimized assistive human–robot interaction using reinforcement learning," *IEEE Trans. Cybern.*, vol. 46, no. 3, pp. 655–667, Mar. 2016.

[16] M. S. Erden and B. Maric, "Assisting manual welding with robot," *Robotics and Computer-Integrated Manufacturing*, vol. 27, no. 4, pp. 818–828, Aug, 2011.

[17] K. H. Lee, S. G. Baek, H. J. Lee, H. R. Choi, H. Moon and J. C. Koo, "Enhanced transparency for physical human-robot interaction using human hand impedance compensation," *IEEE/ASME Trans. Mechatronics*, vol. 23, no. 6, pp. 2662-2670, Dec. 2018.

[18] C. Zeng, C. Yang, J. Zhong and J. Zhang, "Encoding Multiple Sensor Data for Robotic Learning Skills From Multimodal Demonstration," *IEEE Access*, vol. 7, pp. 145604-145613, 2019.

[19] N. Van Toan, J. Kim, K. Kim, W. Lee and S. Kang, "Application of fuzzy logic to damping controller for safe human-robot interaction," in *Proc. 2017 14th International Conference on Ubiquitous Robots and Ambient Intelligence (URAI)*, 2017, pp. 109-113.

[20] S. Barawkar, M. Radmanesh, M. Kumar and K. Cohen, "Fuzzy Logic based Variable Damping Admittance Control for Multi-UAV Collaborative Transportation," in *Proc. 2018 Annual American Control Conference (ACC)*, 2018, pp. 2084-2089.

[21] L. Roveda et al., "Fuzzy Impedance Control for Enhancing Capabilities of Humans in Onerous Tasks Execution," in Proc. 2018 15th International Conference on Ubiquitous Robots (UR), 2018, pp. 406-411.

[22] W. Wang, C. Du, W. Wang and Z. Du, "A PSO-Optimized Fuzzy Reinforcement Learning Method for Making the Minimally Invasive Surgical Arm Cleverer," *IEEE Access*, vol. 7, pp. 48655-48670, 2019.

[23] G. Kang, H. S. Oh, J. K. Seo, U. Kim and H. R. Choi, "Variable admittance control of robot manipulators based on human intention," *IEEE/ASME Trans. Mechatronics*, vol. 24, no. 3, pp. 1023-1032, June 2019.

[24] Y. Li and S. S. Ge, "Human–Robot Collaboration Based on Motion Intention Estimation," *IEEE/ASME Trans. Mechatronics*, vol. 19, no. 3, pp. 1007-1014, June 2014.

[25] M. S. Erden and A. Billard, "Robotic assistance by impedance compensation for hand movements while manual welding," *IEEE Trans. Cybern.*, vol. 46, no. 11, pp. 2459-2472, Nov. 2016.

[26] M. S. Erden and T. Tomiyama, "Human-Intent Detection and Physically Interactive Control of a Robot Without Force Sensors," *IEEE Trans. Robot.*, vol. 26, no. 2, pp. 370-382, April 2010.

[27] F. L. Lewis, S. Jagannathan, and A. Yesildirek, Neural Network Control of Robot Manipulators and Nonlinear Systems. London, U.K.: Taylor & Francis, 1999.

[28] C. Zeng, C. Yang, J. Zhong and J. Zhang, "Encoding Multiple Sensor Data for Robotic Learning Skills From Multimodal Demonstration," *IEEE Access*, vol. 7, pp. 145604-145613, 2019.

[29] X. Chen, N. Wang, H. Cheng and C. Yang, "Neural Learning Enhanced Variable Admittance Control for Human–Robot Collaboration," *IEEE Access*, vol. 8, pp. 25727-25737, 2020.

[30] E. Burdet et al., "A method for measuring endpoint stiffness during multi-joint arm movements," *J. Biomechanics*., vol. 33, no. 12,pp. 1705–1709, 2000.

[31] M. S. Erden and A. Billard, "End-point impedance measurements across dominant and nondominant hands and robotic assistance with directional damping," *IEEE Trans. Cybern.*, vol. 45, no. 6, pp. 1146-1157, June 2015.

[32] M. S. Erden and A. Billard, "End-point impedance measurements at human hand during interactive manual welding with robot," in *Proc. IEEE Int. Conf. Robot. Autom.*, Hong Kong, 2014, pp. 126-133.

[33] T. Tsumugiwa, R. Yokogawa and K. Hara, "Variable impedance control based on estimation of human arm stiffness for human-robot cooperative calligraphic task," in *Proc. IEEE Int. Conf. Robot. Autom.*, vol.1, 2002, pp. 644-650.

[34] Mitra, S., Basak, J. FRBF "A fuzzy radial basis function network," *Neural Computing & Applications*, vol. 10, pp. 244–252, 2001.